Translational Oncology
www.transonc.com

Volume 9 Number 5 October 2016 pp. 419–430 419

Effect of Repeat Dosing of Engineered Oncolytic Herpes Simplex Virus on Preclinical Models of Rhabdomyosarcoma[1]

Alicia M. Waters*, Laura L. Stafman*, Evan F. Garner*, Smitha Mruthyunjayappa*, Jerry E. Stewart*, Gregory K. Friedman†, Jennifer M. Coleman‡, James M. Markert‡, G. Yancey Gillespie‡ and Elizabeth A. Beierle*

*Department of Surgery, Division of Pediatric Surgery, University of Alabama, Birmingham, Birmingham, AL, USA 35233; †Department of Pediatrics, Division of Hematology/Oncology, University of Alabama, Birmingham, Birmingham, AL, USA 35233; ‡Department of Surgery, Division of Neurosurgery, University of Alabama, Birmingham, Birmingham, AL, USA 35233

Abstract

Rhabdomyosarcoma (RMS), a tumor of skeletal muscle origin, is the most common sarcoma of childhood. Despite multidrug chemotherapy regimens, surgical intervention, and radiation treatment, outcomes remain poor, especially in advanced disease, and novel therapies are needed for the treatment of these aggressive malignancies. Genetically engineered oncolytic viruses, such as herpes simplex virus-1 (HSV), are currently being explored as treatments for pediatric tumors. M002, an oncolytic HSV, has both copies of the $\gamma_1$34.5 gene deleted, enabling replication in tumor cells but thwarting infection of normal, postmitotic cells. We hypothesized that M002 would infect human RMS tumor cells and lead to decreased tumor cell survival *in vitro* and impede tumor growth *in vivo*. In the current study, we demonstrated that M002 could infect, replicate in, and decrease cell survival in both embryonal (ERMS) and alveolar rhabdomyosarcoma (ARMS) cells. Additionally, M002 reduced xenograft tumor growth and increased animal survival in both ARMS and ERMS. Most importantly, we showed for the first time that repeated dosing of oncolytic virus coupled with low-dose radiation provided improved tumor response in RMS. These findings provide support for the clinical investigation of oncolytic HSV in pediatric RMS.

Translational Oncology (2016) 9, 419–430

Introduction

Rhabdomyosarcoma (RMS), a malignant neoplasm of striated muscle, is the most common soft tissue sarcoma of childhood. There are two peaks in incidence, between the ages of 2 to 4 and 12 to 16 years, with the majority diagnosed by age 14 years [1]. The most common primary sites include the head, neck, genitourinary tract, and extremities [2]. The World Health Organization categorizes RMS into embryonal, alveolar, spindle/sclerosing, and pleomorphic subtypes, with embryonal RMS accounting for over 70% of cases and representing the most favorable prognosis [3]. The 5-year survival rate in children diagnosed with low-risk RMS is over 90%. Those with metastatic or recurrent disease, however, fare much worse, with a 5-year survival of only 10% to 20% despite aggressive multimodal therapies [4,5]. This is the group which must be targeted for novel therapies.

The Intergroup Rhabdomyosarcoma Study Group, created in 1972, established clinical trials and standard protocols in efforts to improve outcomes and survival [2]. Current treatment regimens for high-risk RMS include surgery, chemotherapy, and radiation therapy [6]. Oncolytic viruses are currently being explored as treatments for

Address all correspondence to: Elizabeth A. Beierle, MD, 1600 7th Ave. South, Lowder Building, Room 300, Birmingham, AL 35233.
E-mail: elizabeth.beierle@childrensal.org
[1] This work was funded in part by a grant from the National Cancer Institute (T32CA091078; to A. M. W., L. L. S., and E. F. G).
Received 23 June 2016; Revised 14 July 2016; Accepted 18 July 2016

1936-5233/16
http://dx.doi.org/10.1016/j.tranon.2016.07.008

pediatric sarcomas [7,8]. M002 is a genetically engineered oncolytic herpes simplex virus (oHSV) with both copies of the $\gamma_1$34.5 gene deleted [9] to decrease neurovirulence [10]. M002 has been shown to have efficacy in pediatric brain tumor [11] and other pediatric solid tumor models [12,13].

These previous results led us to hypothesize that treatment with M002 would result in decreased RMS tumor cell survival *in vitro* and impede tumor growth *in vivo* in an immunocompromised murine model of RMS. Our studies confirmed that M002 had significant cellular effects on two RMS cell lines, including both an embryonal and alveolar model, and decreased RMS xenograft growth *in vivo*. In addition, we have shown for the first time that repeated dosing of an oncolytic virus in combination with irradiation has improved efficacy over single dosing in RMS.

Materials and Methods

Cells and Cell Culture

All cell lines were maintained in standard culture conditions at 37°C and 5% CO_2. RD human embryonal RMS (ERMS) cells (CCL-136; American Type Culture Collection [ATCC], Manassas, VA) were maintained in Dulbecco's modified Eagle's medium containing 10% fetal bovine serum, 4 mM L-glutamine, 1 μM nonessential amino acids, and 1 μg/ml of penicillin/streptomycin. SJCRH30 human alveolar RMS (ARMS) cells (CRL-2061, ATCC) were maintained in RPMI 1640 medium supplemented with 10% fetal bovine serum and 1 μg/ml of penicillin/streptomycin. Vero (ATCC CCL-81, monkey kidney) cells were maintained in Eagle's minimum essential medium with 10% fetal bovine serum. All cell lines were purchased within the last 18 months and were mycoplasma free.

Virus

A genetically engineered oncolytic herpes simplex virus, M002, has been previously described [9]. Briefly, R3659 was the parent virus for M002 with the thymidine kinase gene inserted into deleted regions of both $\gamma_1$34.5 loci and a deletion in the native thymidine kinase locus. M002 is a conditionally replication-competent mutant herpes simplex virus expressing both subunits of murine interleukin-12 (mIL-12) under the transcriptional control of the murine early-growth response-1 promoter; two copies of the entire construct are present, with a single copy inserted into each of the $\gamma_1$34.5 loci; the native thymidine kinase gene is restored. To titer the M002 virus, Vero cells were plated in 24 well plates at 1.5×10^5 cells per well and allowed 24 hours to attach and form a confluent monolayer. Ten-fold dilutions of stock virus in infection medium (1% FBS in Dulbecco's modified Eagle's medium/F12) were applied to the Vero cells for 2 hours, the inoculum was removed, and the plates were washed with media. After 48 hours of incubation, May-Grunwald stain in methanol was applied for 20 minutes, and plates were washed and dried overnight. Plaques were counted, and the titer was calculated and reported as plaque-forming units per milliliter (PFU/ml).

Viral Replication

Viral recovery experiments were performed as described previously [12,13]. For single-step viral recovery, RD and SJCRH30 cells were plated and allowed to attach for 24 hours. The cells were infected with M002 at a multiplicity of infection (MOI) of 10 PFU/cell for 2 hours. After 12 and 24 hours, the cells were harvested by adding equal volume of sterile milk and freezing at −80°C. Plates were thawed at 37°C and underwent two more freeze/thaw cycles. Cells and supernates were collected, milk stocks were sonicated for 30 seconds, and the titers of progeny virions were determined on Vero cell monolayers. The average PFU/ml was calculated from quadruplicate wells.

For multistep viral recovery experiments, RD and SJCRH30 cells were grown to confluence in six-well plates and then infected with M002 at an MOI of 0.1 PFU/cell. The media from the cells were harvested at 6, 24, 48, and 72 hours postinfection. The titers of progeny virions in the supernate were determined as above, and the average PFU/ml was calculated from quadruplicate wells.

ELISA

Production of mIL-12 by the recombinant M002 virus was quantified using a total mIL-12 ELISA kit (Thermo Fisher Scientific, Rockford, IL). Ninety-six–well plates were seeded with 1.5×10^4 cells per well for 24 hours and then treated with media alone or M002. After incubating for 48 hours, the supernates were collected and analyzed by ELISA according to the manufacturer's protocol.

Virus Cytotoxicity Assays

Cell viability 72 hours after virus treatment *in vitro* was measured using an alamarBlue assay. Cells were plated (1.5×10^3 cells/100-μl well) in 96-well culture plates and after 24 hours were treated with 100 μl of saline or a graded series of dilutions of M002. After 72 hours of culture, 10 μl of sterile alamarBlue dye (Invitrogen Life Technologies, Grand Island, NY) was added to each well. After 4 to 6 hours, the absorbance at 542 and 595 nm was measured using a kinetic microplate reader (BioTek Gen5; BioTek Instruments, Winooski, VT). Virus cytotoxicity at each dilution was measured by the reduction in the color change compared with that seen in the saline treatment group (100%) viability. These values were plotted to yield an estimate of the PFU of M002 required to inhibit 50% of the cells by 72 hours (IC_{50}/PFU).

Antibodies

Antibodies used for Western blotting were as follows: rabbit polyclonal anti-PVRL-1 (CD111) from Abcam (ab71512; Abcam, Cambridge, MA); rabbit polyclonal anti-nectin 2 (CD112) from Bioss (bs2679R; Bioss Inc., Woburn, MA); rabbit polyclonal anti-syndecan-2 from LS Biosciences (LS-B2981; LifeSpan Biosciences, Inc., Seattle, WA); rabbit polyclonal anti-phospho Stat1 (Y701, 9171S), anti-Stat1 (9172S), mouse monoclonal anti-phospho p38 mitogen-activated protein kinase (MAPK) (Thr180/Tyr182, 9216S), and rabbit polyclonal anti-PARP (9542S) from Cell Signaling (Cell Signaling Technology, Inc., Danvers, MA); and rabbit polyclonal anti-p38 (H-147, sc-7149) from Santa Cruz (Santa Cruz Biotechnology Inc., Santa Cruz, CA). Mouse monoclonal anti–β-actin (a1978) was purchased from Sigma (Sigma-Aldrich, St. Louis, MO).

Western Blotting

Western blots were performed as previously described [14]. Cells were lysed on ice for 30 minutes in a buffer containing 50 mM Tris–HCL (pH 7.5), 150 mM NaCl, 1% Triton-X, 0.5% NaDOC, 0.1% SDS, 5 mM EDTA, 50 mM NaF, 1 mM NaVO3, 10% glycerol, and protease inhibitors: 10 μg/ml of leupeptin, 10 μg/ml of PMSF, and 1 μg/ml of aprotinin. The lysates were cleared by centrifugation at 14,000 rpm for 30 minutes at 4°C. Protein concentrations were determined using a Bio-Rad kit (Bio-Rad, Hercules, CA), and

proteins were separated by electrophoresis on SDS-PAGE gels. Antibodies were used according to manufacturers' recommended conditions. Molecular weight markers (Bio-Rad) were used to confirm the expected size of the target proteins. Immunoblots were developed with chemiluminescence (Amersham ECL; GE Healthcare Biosciences, Pittsburgh, PA). Blots were stripped with stripping solution (Bio-Rad) at 37°C for 15 minutes, rinsed, and then reprobed with selected antibodies. Immunoblotting with antibody to anti–β-actin provided an internal control for equal protein loading.

Apoptosis

Cellular apoptosis was detected with two methods; immunoblotting for PARP cleavage and a commercially available colorimetric caspase 3 activation kit (KHZ0022; Invitrogen, Life Technologies, Thermo Fisher Scientific, Inc.). For immunoblotting, cells were treated with increasing MOI of M002 and whole cell lysates utilized for SDS-PAGE. Membranes were probed with appropriate antibodies with β-actin serving as an internal control for equal protein loading. Increasing intensity of PARP bands for cleaved products combined with decreasing intensity of bands for total PARP indicated apoptosis. Additionally, activation of caspase 3 was also measured with a kit, according to manufacturer's instructions.

Immunohistochemistry

Human specimens were obtained following institutional review board (IRB) approval (X100930009) under a waiver of informed consent, and all experiments were carried out in accordance with the IRB-approved guidelines. Formalin-fixed, paraffin-embedded tumor blocks of murine xenografts or human RMS specimens were cut in 8-μm sections. The slides were baked for 1 hour at 70°C, deparaffinized, rehydrated, and steamed. The sections were then quenched with 3% hydrogen peroxide and blocked with PBS-blocking buffer. The primary rabbit polyclonal antibody, anti–herpes simplex virus type I antibody (1:250, PU084-UP; BioGenex, Fremont, CA), or primary mouse polyclonal anti-CD111 antibody (1:300, ab66985, Abcam) was added and incubated overnight at 4°C. After washing the HSV slides with PBS, the Superpicture anti-rabbit HRP secondary antibody (Life Technologies, Inc., Grand Island, NY) was added at 1:250 dilution for 1 hour at 22°C. The staining reaction was developed with VECTASTAIN Elite ABC kit (PK-6100; Vector Laboratories, Burlingame, CA), TSA (biotin tyramide reagent, 1:400; PerkinElmer, Inc., Waltham, MA), and DAB (Metal Enhanced DAB Substrate; Thermo Fisher Scientific). For the CD111 slides, after washing with PBS, the Super Sensitive Polymer-HRP Detection Kit with DAB (QD400-60K; Biogenex, Fremont, CA) was utilized for detection of the antigen-antibody binding. Slides were counterstained with hematoxylin. A negative control (rabbit IgG or mouse IgG, 1 μg/ml [Millipore, EMD Millipore, Billerica, MA]) was included with each experiment. For hematoxylin and eosin staining, slides were cut and baked as described above, and standard hematoxylin and eosin staining methods were utilized.

Immunohistochemistry Scoring

Staining for HSV-1 in xenograft tumors was quantified by ImageJ software (http://rsb.info.nih.gov/ij/). Positive HSV-1 staining was reported as percent positive staining cells per high-power field after counting 10 random fields of view per specimen. CD111 staining in human RMS specimens was quantified by pathologist (S. M.) blinded to the specimens. Specimens were scored based upon the intensity of staining and the percentage of tumor cells staining. Intensity was graded from 0 to 3 (0, none; 1, weak; 2, moderate; 3, strong) and multiplied by the percentage of cells with that staining. For example, if the specimen showed moderate staining (2) in 40% of the cells, the stain score would be 80 (2 × 40 = 80).

Tumor Growth In Vivo

Animal experiments were completed following institutional institutional animal care and use committee (IACUC) approval (IACUC-09363). Six-week-old female athymic nude mice were purchased from Harlan Laboratories, Inc. (Chicago, IL). The mice were maintained in the specific pathogen free (SPF) animal facility with standard 12-hour light/dark cycles and allowed chow and water *ad libitum*. All experiments were carried out in accordance with the approved guidelines, and at the completion of the experiments, euthanasia was accomplished according to American Association for Laboratory Animal Science guidelines utilizing compressed CO_2 gas in their home cage followed by bilateral thoracotomy. Human RMS cells, RD (2.5×10^6 cells), and SJCRH30 (2.0×10^6 cells) in Matrigel (1:1 dilution with sterile PBS, volume 100 μl; BD Biosciences, San Jose, CA) were injected subcutaneously into the right flank. Once tumors reached approximately 250 mm^3, animals (n = 40) were randomized to receive an intratumoral injection of vehicle (PBS + 10% glycerol, 50 μl) or M002 virus (1×10^7 PFU/50 μl) (n = 20). These concentrations were chosen based upon previous investigations with the virus [9,12,13]. Within 6 hours of treatment, half of the vehicle-treated tumors and half of the M002-treated tumors received a low dose of external beam irradiation (3 Gy) directed at the flank tumor (n = 10 animals/group). Previous studies have demonstrated the enhanced oncolytic effects of viral therapy when combined with radiation [15]. Tumors were measured twice weekly with a caliper, and tumor volume in mm^3 was calculated using a standard formula [(width^2 × length)/2], where width was the smaller diameter. Once tumors reached the size predetermined by IACUC protocol standards, the animals were euthanized, and the tumors were harvested and processed for study.

For the repeated-dosing study, ARMS SJCRH30 cell line was chosen because ARMS tends to be more difficult to treat than ERMS. SJCRH30 (2.0×10^6) cells in Matrigel (1:1 dilution with sterile PBS, volume 100 μl; BD Biosciences) were injected subcutaneously into the right flank of 6-week-old female nude mice (n = 20). Once tumors reached approximately 250 mm^3, animals were randomized to receive a single intratumoral injection of M002 virus (1×10^7 PFU/50 μl) (n = 6) or an additional two intratumoral doses of virus (1×10^7 PFU/50 μl, total of three doses) at 3-day intervals with (n = 7) or without the addition of low-dose flank irradiation (XRT) (n = 7) following the virus injection. Tumors were measured twice weekly with a caliper, and tumor volume in mm^3 was calculated using a standard formula [(width^2 × length)/2], where width was the smaller diameter. Once tumors reached the size predetermined by IACUC protocol standards, the animals were euthanized.

Data Analysis

Experiments were repeated at least in triplicate, and data are reported as mean ± standard error of the mean. An analysis of variance or Student's t test was used as appropriate to compare data between groups, and log-rank test was used to determine survival significance. Statistical analyses were completed using SigmaPlot 12 software (SyStat Software, Inc., San Jose, CA) with statistical significance determined at the $P \leq .05$ level.

Results

HSV Entry Receptors and Viral Infectivity

Two different histologic subtypes of RMS were chosen for study: ERMS (RD) and ARMS (SJCRH30) [16]. CD111 (poliovirus receptor-related protein 1 [nectin-1]) is a cell surface receptor that is the primary viral entry mediator used by HSV-1 for cellular entry [17]. Immunoblotting with CD111 specific antibody detected CD111 protein in whole cell lysates of SJCRH30 and RD RMS cells lines (Figure 1*A*). Two additional virus entry receptors were also investigated. It has been reported in the literature that certain laboratory strains of HSV-1 may use CD112 (poliovirus receptor-related 2, nectin-2) as another receptor for cell entry [18,19], so we also examined cell lysates for this protein and found that CD112 was also expressed by the SJCRH30 and RD cell lines (Figure 1*B*). Additionally, heparin sulfate proteoglycan (syndecan-2) is another protein known to play an important role in HSV-1 viral entry and spread [20]. Cell lysates from SJCRH30 and RD cells were examined with immunoblotting and found to have syndecan-2 protein present (Figure 1*C*). These data indicated that these cell lines had the receptors necessary for HSV-1 viral entry and infection.

In anticipation of advancing to human studies and to provide a rationale for clinical application of oHSV for RMS, we determined whether CD111 protein was present in human RMS specimens. Following IRB approval (X100920009) under a waiver of informed consent, we performed CD111 immunostaining on human ERMS (n = 12) and ARMS (n = 10) specimens. The CD111 staining was scored by a pathologist (S. M.) blinded to the specimens, and the mean stain scores were compiled based upon stain intensity. CD111 staining was positive in all of the specimens examined, with a mean stain score of 89 ± 2% in ARMS and 91 ± 1% in ERMS specimens. Representative photomicrographs were presented at 10× and 40× (Figure 1, *D* and *E*). There was cell surface CD111 staining in both tumor types (Figure 1, *D* and *E*, *black arrows*), and negative controls (rabbit IgG) reacted appropriately (Figure 1, *D* and *E*, *small box inserts*).

To ascertain whether M002 could infect and replicate in the RMS cell lines, *in vitro* replication of M002 was evaluated in the RD and SJCRH30 cell lines using single- and multistep viral recovery experiments. For the single-step experiments, the RD and SJCRH30 cell lines were infected with M002 at an MOI of 10 PFU/cell. By 24 hours postinfection, there were significant viral titers noted in both cell lines (Figure 2*A*) that continued to increase at 48 hours postinfection (Figure 2*A*). For multistep viral recovery, monolayers of RD and SJCRH30 cell lines were infected with M002 at an MOI of 0.1 PFU/cell, and at 6, 24, 48, and 72 hours postinfection, viral

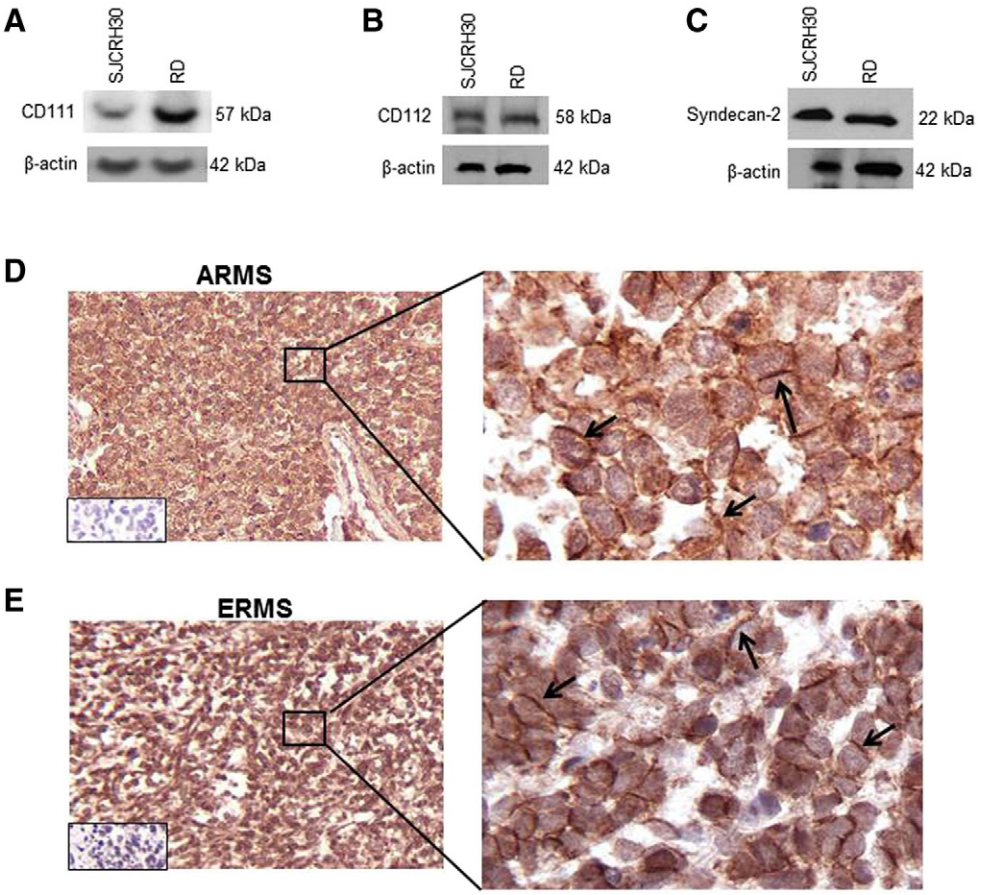

Figure 1. HSV entry receptors in cell lines and human RMS specimens. (A–C) Immunoblotting with CD111, CD112, and syndecan-2 specific antibodies demonstrated all three proteins to be present in whole cell lysates of SJCRH30 and RD human RMS cell lines. β-Actin was used to confirm equal protein loading. Immunohistochemical staining was performed on human ARMS (D) and ERMS (E) specimens. Representative photomicrographs at 10× and 40× are presented. There was CD111 staining present on the cell surface (*black arrows*) in both histologic types. Negative controls reacted appropriately (*bottom left inserts,* D, E).

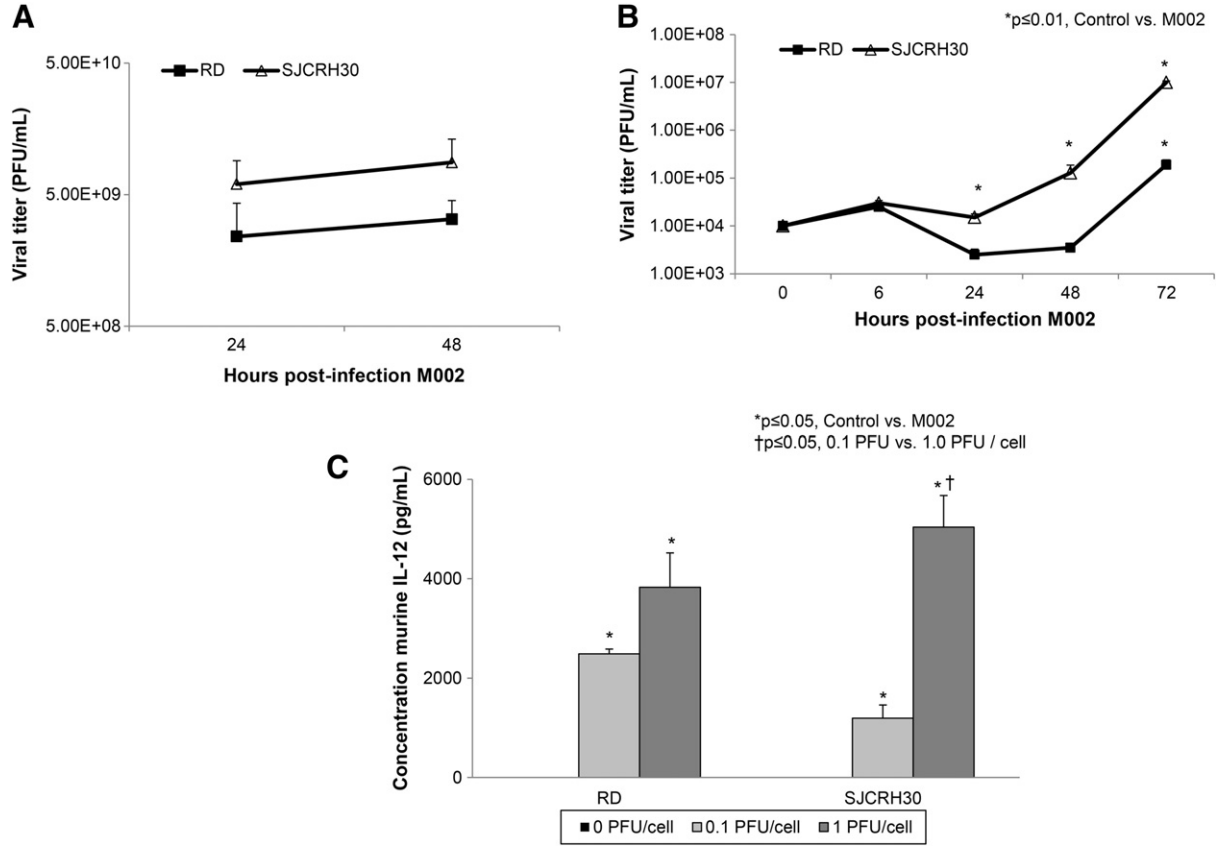

Figure 2. Infectivity of M002 in RMS cell lines. (A) Single-step *in vitro* replication of M002. Monolayers of RD and SJCRH30 cells were infected with M002 at an MOI of 10 PFU/cell. Replicate cultures were harvested at 24 and 48 hours postinfection, and virus titers were determined on Vero cell monolayers. Mean virion yields were determined in four replicates at each time point, and standard error of the mean was determined. By 24 hours postinfection, there were significant viral titers noted in both cell lines that continued to increase at 48 hours postinfection. (B) Multistep replication of M002. Monolayers of RD and SJCRH30 cells were infected with M002 at an MOI of 0.1 PFU/cell, and at 6, 24, 48, and 72 hours postinfection, supernates were collected, and virus titers were determined on Vero cell monolayers. Mean virion yields were determined in four replicates at each time point, and standard error of the mean was determined. In the RD cell line, M002 replicated more than a log higher than control at 72 hours postinfection, and in the SJCRH30 cell line, replication of virus was more than 3 logs greater than time zero. (C) Because M002 was engineered to produce mIL-12, to further verify infection, mIL-12 production was determined in RD and SJCRH30 cell lines following treatment with M002 oHSV. Cell lines were infected with M002 at 0, 0.1, or 1.0 PFU/cell. At 48 hours postinfection, the supernates were collected, and concentrations of mIL-12 were determined by ELISA. Data are reported as mean ± standard error of the mean. There was a significant increase in mIL-12 production in both cell lines even with the lower MOI of virus.

replication was determined. As shown in Figure 2*B*, after 72 hours of infection, M002 replicated to a titer significantly higher in both cell lines compared with that of time zero.

Because M002 was genetically engineered to produce mIL-12, to further verify viral infection, we sought to determine the extent to which the infected human RMS cell lines would produce the encoded foreign mIL-12 protein. The RD and SJCRH30 cells were infected with M002 at 0, 0.1, or 1.0 PFU/cell. After 24 hours of infection, the supernates were collected, and an mIL-12 ELISA kit was utilized to detect IL-12 production. There were significant increases in mIL-12 after M002 infection of both RMS cell lines (Figure 2*C*), confirming infection and virus replication in both cell lines. In the RD cell line, infection with 0.1 PFU/cell for 24 hours resulted in a concentration of mIL-12 of 2486 ± 100 pg/ml, significantly greater than the concentration after infection with 0 PFU/cell (control, 0.0 pg/ml, $P = .002$) (Figure 2*C*). Similar findings were seen with the SJCRH30 cell line; infection with 0.1 PFU/cell for 24 hours resulted in a concentration of mIL-12 of 1194 ± 265 pg/ml, significantly greater than concentration of 0.0 pg/ml after infection with 0 PFU/cell (control, $P = .04$) (Figure 2*C*). In addition, in the SJCRH30 alveolar cell line, increasing the MOI of the M002 oHSV by a factor of 10 resulted in a statistically significant increase in the production of mIL-12 compared with the lower MOI (1194 ± 265 pg/ml vs 5036 ± 636 pg/ml, 0.1 PFU/cell vs 1.0 PFU/cell, $P = .03$). Previous studies from our group have shown that the parent virus, devoid of mIL-12 insertion, does not stimulate mIL-12 production in human cell lines [9]. The ELISA studies were utilized only to verify virus infection.

Treatment with M002 Resulted in Cell Death

RMS cell lines (RD, SJCRH30) were treated for 72 hours with M002 at increasing concentrations (0-20 PFU/cell), and cell viability was measured with alamarBlue assays. Both cell lines had a significant decrease in viability following M002 treatment (Figure 3*A*). The lethal dose of virus that resulted in 50% killing (LD_{50}) for the embryonal RD cells was 3.3 ± 0.1 PFU/cell and for the alveolar SJCRH30 cells was 4.1 ± 0.4 PFU/cell.

Next, we investigated whether the viral-induced cell death was due to apoptosis. RD and SJCRH30 cell lines were treated with increasing concentrations of M002 (0-10 PFU/cell), and whole cell lysates were collected after 72 hours of treatment. Lysates were studied with immunoblotting to detect cleavage of PARP. The decrease in total PARP, accompanied with an increased in the cleaved PARP product, indicated that the RMS cells were undergoing apoptosis. This finding was evident in both cell lines (Figure 3*B*). Apoptosis was confirmed using a caspase 3 activation kit. There was a significant increase in caspase 3 activation in the SJCRH30 cell line at 0.1 PFU/cell and in the RD cell line at MOI of 10 PFU/cell (Figure 3*C*), similar to the results seen in the PARP immunoblotting, indicating an apoptotic process.

In Vivo Tumor Studies

All experiments were performed in accordance with relevant guidelines and regulations after IACUC approval (IACUC-09,363). To determine the *in vivo* effects of M002 treatment on RMS, nude mouse xenograft models were utilized. RD human ERMS cells (2.5×10^6 in Matrigel [BD Biosciences]) were injected subcutaneously into the right flank of female athymic nude mice ($n = 40$). Once flank tumors reached an average volume of 250 mm^3, the tumors were injected with either control vehicle (PBS + glycerol, 50 µl, $n = 20$) or a single dose of M002 (1×10^7 PFU/50 µl, $n = 20$). Because the addition of low dose radiation has been shown to increase the activity of oHSV in malignant gliomas [15,21,22], we examined whether the addition of a single low dose of radiation would also enhance the efficacy of M002 in the RD xenografts. Therefore, half of the animals in each group received a low dose of irradiation to the tumor immediately following injection with vehicle or M002. Three grays (3 Gy, XRT) was chosen because other investigations have shown that HSV replication increased in a dose-dependent fashion following irradiation with 2 to 5 Gy, with no additional effects seen after 5 Gy [22]. Tumor volumes were measured biweekly with calipers. Tumor volumes were followed 40 days, when most of the vehicle-treated animals had been euthanized as dictated by IACUC protocol. In the animals treated with M002 and XRT, there was a significant decrease in tumor growth beginning at day 19 and continuing to 40 days when compared with the animals in the vehicle or vehicle + XRT treatment groups ($P \leq .05$) (Figure 4*A*). Tumor volumes in the M002 + XRT were also smaller than those from M002 alone but did not reach statistical significance. The addition of low-dose (3 Gy) XRT to the vehicle treatment did not significantly affect tumor growth when compared with vehicle alone (Figure 4*A*). Animals were followed for

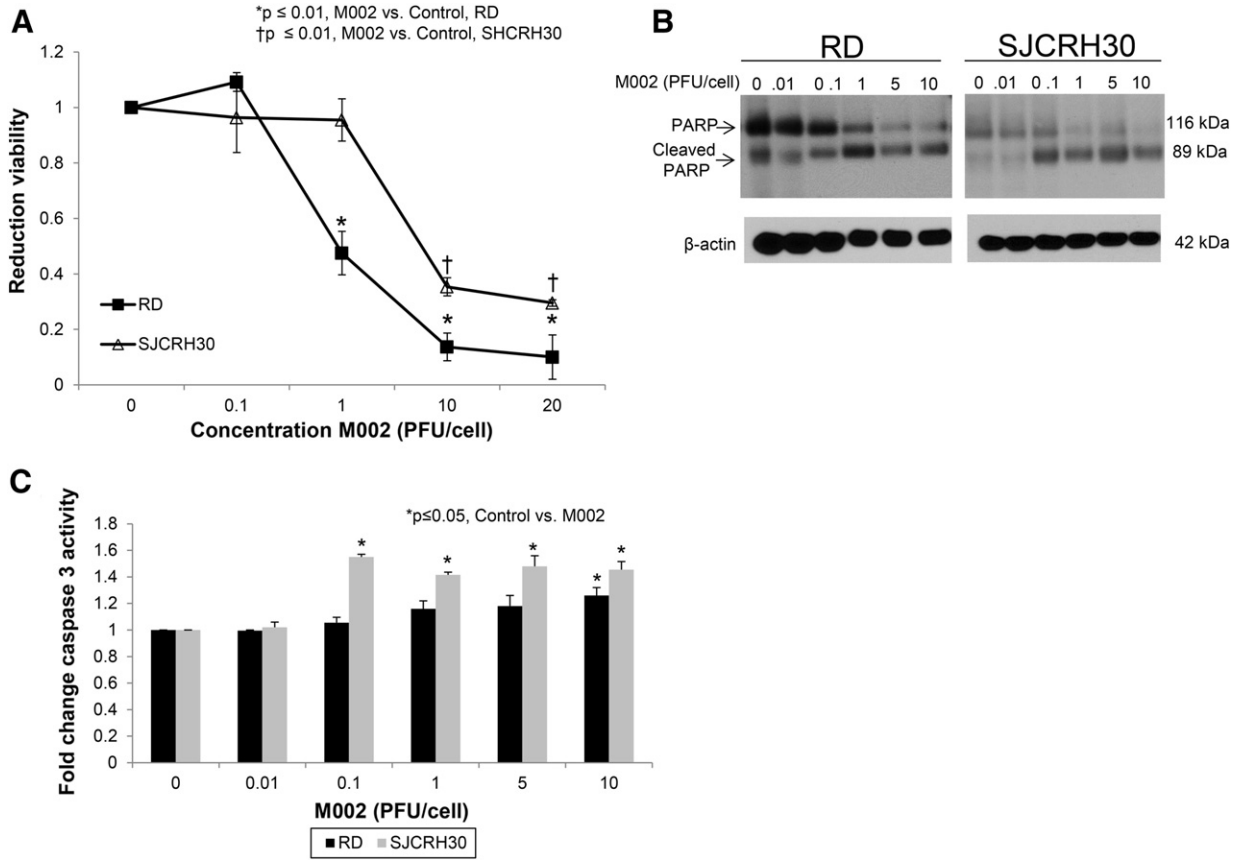

Figure 3. Treatment with M002 resulted in cell death. (A) RD and SJCRH30 cell lines were treated with M002 at increasing MOI. After 72 hours of treatment, cell viability was measured with alamarBlue assays. Data are reported as mean ± standard error of the mean. There was a significant decrease in viability in both cell lines following M002 treatment. The LD_{50} was calculated for each cell line for M002 and was 3.3 ± 0.1 PFU/cell for embryonal RD cells and 4.1 ± 0.4 PFU/cell for the alveolar SJCRH30 cells. (B) To determine whether RMS cells were undergoing an apoptotic process following M002 treatment, immunoblotting for cleavage of PARP was completed. There were a significant decrease in total PARP staining and an increase in cleaved PARP staining in both cell lines with increasing MOIs. (C) To further verify apoptosis, a caspase 3 activation kit was utilized. There was a significant increase in caspase 3 activation following M002 treatment, indicating that the RMS cells were undergoing an apoptotic process.

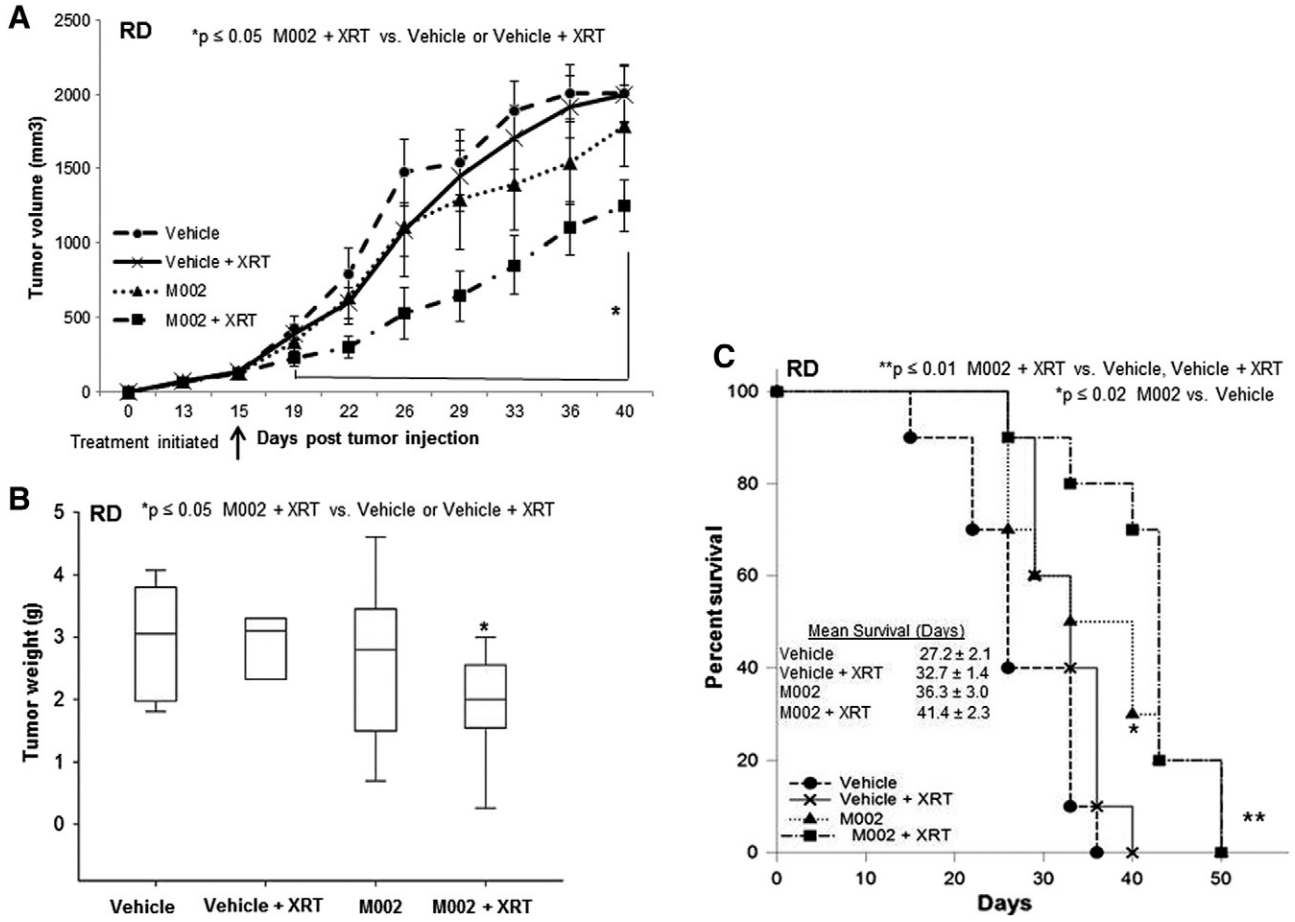

Figure 4. M002 treatment of RD xenografts. (A) RD human RMS tumor cells (2.5×10^6 cells) were injected into the right flank of athymic nude mice. Once tumors reached a volume of 250 mm^3, animals received an intratumoral injection of vehicle (PBS+ 10% glycerol, 50 μl [$n = 20$]) or M002 virus (1×10^7 PFU/50 μl [$n = 20$]). Half of the animals in each group also received low-dose irradiation (3 Gy) at the time of injection. Tumor volumes were measured twice weekly [(width)2 × length]/2 for 40 days. Data are reported as tumor volume ± standard error mean. In the animals treated with M002 and XRT, there was a significant decrease in tumor growth beginning at day 19 when compared with the animals in the vehicle or vehicle + XRT treatment groups. Tumor volumes in the M002 + XRT were also smaller than those from M002 alone, but this did not reach statistical significance. The addition of low-dose (3 Gy) XRT to the vehicle treatment did not significantly affect tumor growth (Figure 3*A*). (B) Xenograft tumors were weighed at euthanasia. There was a significant decrease in tumor weight in the animals treated with M002 and XRT when compared with animals that received vehicle alone or vehicle with XRT. Tumor weights in M002 + XRT group tended to be less than those of M002 alone but did not reach statistical significance. Lines in bars represent the median, and the whiskers represent the 5th and 95th percentile. (D) Kaplan-Meier curves were constructed with log-rank statistics to evaluate animal survival. Animals treated with M002 had significantly increased survival over those treated with vehicle alone. Animals treated with M002 + XRT also had a significant survival advantage when compared with those treated with vehicle or vehicle +XRT.

survival, and tumors were weighed at the time of euthanasia. RD xenograft tumors treated with M002 + XRT weighed significantly less than those treated with vehicle or vehicle + XRT (1.9 ± 0.3 g vs 3 ± 0.3 g or 2.8 ± 0.3 g, M002 + XRT versus vehicle or vehicle + XRT, $P \leq .02$) (Figure 4*B*). The M002 + XRT tumors also weighed less than those treated with M002 alone but, similar to tumor volume, did not reach significance (Figure 4*B*). There were some differences in the final weights of the animals at the time of euthanasia, but these were not statistically significant (Figure S1*A*). To exclude animal growth as an explanation for differences in tumor weights, tumor to body weight ratios at the time of animal euthanasia were calculated. These ratios (Figure S1*B*) were consistent with the data seen with tumor weights alone, discounting animal growth as a factor in tumor weight differences. As seen in Figure 4*C*, the animals treated with M002 had significantly increased survival when compared with vehicle-treated animals (36.3 ± 3.0 vs 27.2 ± 2.1 days, M002 versus vehicle, $P = .017$). In addition, animals treated with M002 + XRT had significantly increased survival over those treated with vehicle or vehicle + XRT (Figure 4*C*).

The second set of *in vivo* experiments examined the effects of M002 upon SJCRH30 ARMS xenografts. SJCRH30 cells (2.0×10^6 cells in Matrigel [BD Biosciences]) were injected into the subcutaneous space of the right flank of female nude mice ($n = 40$). Once xenografts reached 250 mm^3, tumors were injected with vehicle (PBS + glycerol, 50 µl, $n = 20$) or a single dose of M002 (1×10^7 PFU/50 µl, $n = 20$). Half of the animals in each group received a single low dose of external beam irradiation (3 Gy, XRT) to the tumor as described above. Tumor volumes were followed for 41 days when most of the vehicle-treated animals had been euthanized per IACUC protocol. Animals treated with M002 + XRT had

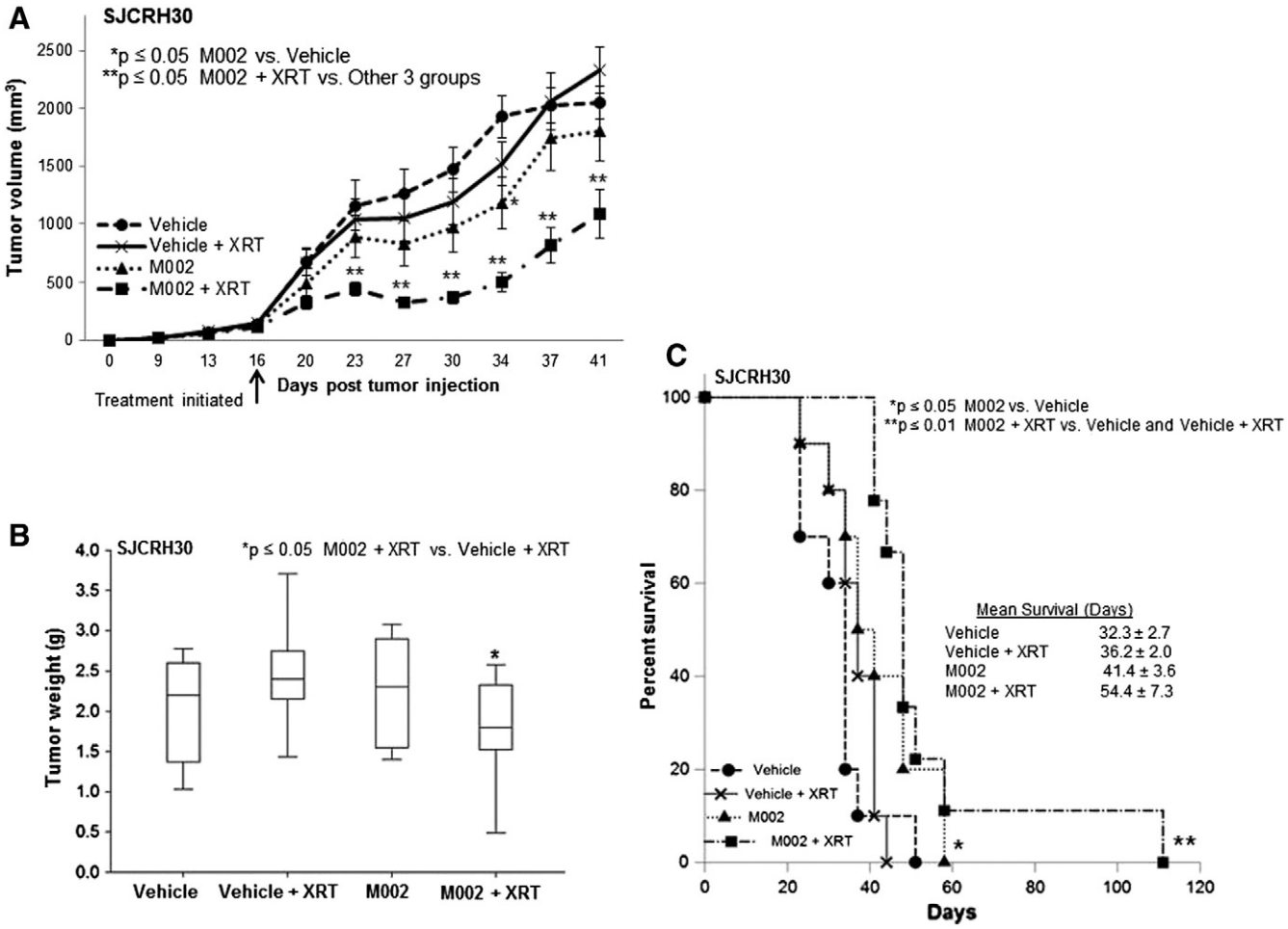

Figure 5. M002 treatment of SJCRH30 xenografts. (A) SJCRH30 cells (2.0×10^6 cells) were injected into the subcutaneous space of the right flank of female nude mice ($n = 40$). Once tumors reached 250 mm^3, animals received an intratumoral injection of vehicle (PBS+ 10% glycerol, 50 μl [$n = 20$]) or M002 virus (1×10^7 PFU/50 μl [$n = 20$]). Half of each group was also treated with 3-Gy external beam radiation at the time of injection (XRT). Tumor volumes were measured twice weekly and reported as tumor volume ± standard error. Beginning on day 23, there was a significant decrease in tumor volume in the animals treated with combined M002 + XRT. (B) Xenograft tumors were weighed at euthanasia. There was a significant decrease in tumor weight in the animals treated with M002 and XRT when compared with animals that received vehicle with XRT. Lines in bars represent the median, and the whiskers represent the 5th and 95th percentile. (C) Kaplan-Meier curves were constructed with log-rank statistics to examine animal survival. Animals treated with M002 had significantly increased survival over those treated with vehicle alone. Animals treated with M002 + XRT also had a significant survival advantage when compared with those treated with vehicle or vehicle and XRT.

significantly smaller tumor volumes than the animals from the other three treatment groups, including M002 alone (Figure 5*A*). The addition of low-dose (3 Gy) XRT to the vehicle treatment did not affect SJCRH30 tumor growth compared with vehicle alone (Figure 5*A*). The animals remaining were followed for survival. At euthanasia, tumors were harvested and weighed. M002 + XRT–treated SJCRH30 xenografts tended to weigh less than those of the other treatment groups, but this difference reached statistical significance only when compared with the vehicle + XRT treatment group (Figure 5*B*). As seen with the RD xenografts, there were some differences in the final weights of the animals at the time of euthanasia, but these were not statistically significant (Figure S1*C*). Tumor to body weight ratios at the time of animal euthanasia were calculated, and these ratios (Figure S1*D*) were consistent with the data seen with tumor weights alone, discounting animal growth as a factor in tumor weight differences. Animals treated with M002 alone had improved mean survival over animals treated with vehicle alone (41.4 ± 3.6 vs 32.3 ±2.7 days, M002 versus vehicle, $P = .05$) as depicted in Figure 5*C*. Furthermore, animals treated with M002 + XRT had an increase in survival over those treated with vehicle alone or with vehicle + XRT (Figure 5*C*). The notable decreases in tumor volume with the addition of XRT to M002 treatment (Figure 5*A*) did not translate into statistically improved survival advantage over M002 alone (54.4 ± 7.3 vs 41.4 ± 3.6 days, $P = .3$, M002 + XRT versus M002, Figure 5*C*). In both cell types, tumor growth was significantly decreased but not completely abrogated.

The presence of HSV in the tumors following treatment was verified with immunohistochemical staining for HSV-1. Representative photomicrographs are presented in Figure 6. Immunohistochemical staining for HSV-1 detected virus in tumors injected with M002 (Figure 6, *middle panel brown stain, white arrows*) and with M002 + XRT (Figure 6, *lower panel brown stain, white arrows*) for up to 7 days post virus injection. There was a lack of staining in tumors injected with vehicle (Figure 6, *upper panel*). Negative controls

reacted appropriately (Figure 6, *insert bottom right upper, middle, and lower panels*). Immunohistochemical staining was quantified with ImageJ software. There was a slight increase in the amount of positive staining at 7 days postinfection when comparing tumors treated with M002 + XRT versus those treated with M002 alone, but this finding was not statistically significant.

Because M002 did not result in a sustained response in decreasing tumor growth, we advanced to a model of repeated dosing of virus. We chose to study the SJCRH30 cell line because ARMS is clinically more difficult to treat. SJCRH30 cells (2.0×10^6 cells in Matrigel [BD Biosciences]) were injected into the subcutaneous space of the right flank of female nude mice ($n = 20$). Once xenografts reached

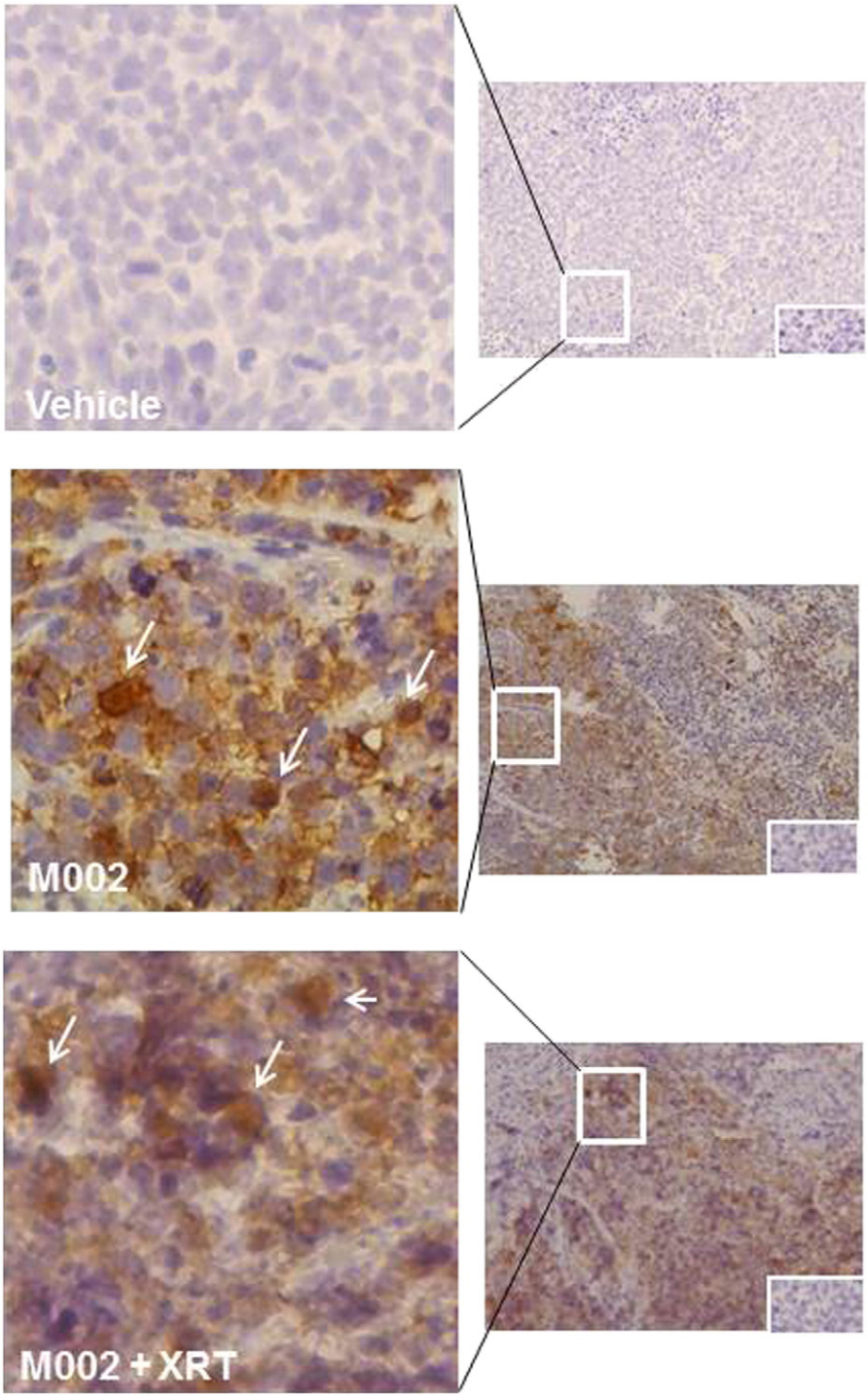

Figure 6. Histological examinations of RMS xenografts for HSV. The presence of HSV in the tumors following treatment was verified with immunohistochemical staining for HSV-1. Representative photomicrographs are at 20× (*right*) and 40× (*left*). Immunohistochemical staining for HSV-1 detected virus in tumors injected with M002 (*middle panels brown stain, white arrows*) and M002 + XRT (*bottom panels brown stain, white arrows*), present at 7 days post virus injection. Tumors injected with vehicle did not demonstrate HSV staining (*upper panels*). Negative controls reacted appropriately (*insert, bottom right, upper, middle, and lower panels*).

250 mm^3, animals were randomized to three treatment groups: 1) a single intratumoral injection of M002 on day 0 (1×10^7 PFU/50 µl, $n = 6$); 2) repeated intratumoral injection of M002 on days 0, 3, and 6 (1×10^7 PFU/50 µl, $n = 7$); or 3) repeated intratumoral injection of M002 (1×10^7 PFU/50 µl) on days 0, 3, and 6 with low-dose XRT (3 Gy) on those days ($n = 7$). Tumor volumes were measured twice weekly and followed for 40 days when most of the single-dose animals had been euthanized per IACUC protocol. Animals treated with repeated doses of M002 had significantly smaller tumor volumes than the animals that received only a single dose of virus (Figure 7). Furthermore, animals that were given low-dose XRT in addition to repeat M002 had smaller tumors than those that did not receive additional XRT and those that had only a single intratumoral injection of M002 (Figure 7).

STAT1 and p38 MAPK

We investigated possible mediators of sensitivity of the two RMS cell lines to M002. Previous investigators have shown that upregulation of STAT1 was associated with decreased response to oHSV [23]. Other investigators have shown that decreased phosphorylation of p38 was also associated with resistance to oHSV and that increased activation of p38 MAPK was associated with improved virus replication [21,23,24]. Therefore, to determine if these proteins played a potential role in the difference in responses of the cell lines to oHSV, immunoblotting was utilized to determine their expression and phosphorylation. STAT1 activation did not increase following M002 treatment in either cell line (Figure S2*A*), and p38 phosphorylation appeared to increase with M002 treatment in both cell lines (Figure S2*B*).

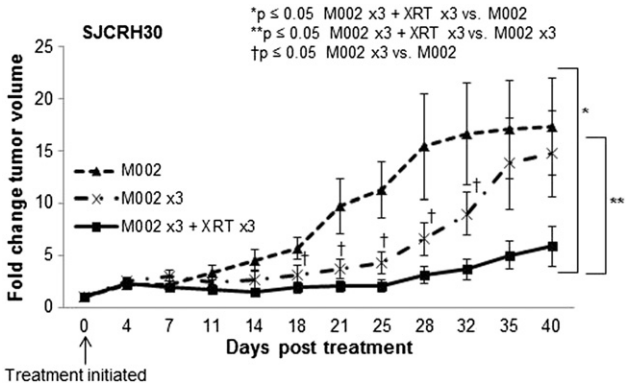

Figure 7. Repeated injections of M002 in SJCRH30 xenografts. SJCRH30 cells (2.0×10^6 cells) were injected into the subcutaneous space of the right flank of female nude mice ($n = 20$). Once tumors reached 250 mm^3, animals were randomized to three groups: 1) single intratumoral injection of M002 virus (1×10^7 PFU/50 µl [$n = 6$]); 2) repeated intratumoral injection of M002 (1×10^7 PFU/50 µl) on days 0, 3, and 6 ($n = 7$); and 3) repeated intratumoral injection of M002 (1×10^7 PFU/50 µl) followed by low-dose irradiation (3 Gy, XRT) on days 0, 3, 6 and ($n = 7$). Tumor volumes were measured twice weekly and reported as fold change in tumor volume ± standard error. Beginning on posttreatment day 18, the animals receiving multiple doses of M002 had significantly less tumor growth than those treated with a single dose. The animals treated with multiple doses of M002 and XRT had significantly less tumor growth than either the single M002 dose or those that received multiple doses of M002 without XRT.

Discussion

Despite therapeutic advances in the treatment of RMS, advanced stage and recurrent tumors continue to carry a dismal prognosis with little chance for long-term survival. Clearly, novel therapeutic interventions are needed to combat this cancer, and various virotherapies including vaccinia virus, picornavirus, and herpes simplex viruses have been investigated as alternative treatments for these tumors. He and colleagues utilized a recombinant vaccinia oncolytic virus and demonstrated 40% cytotoxicity in the RMS cell line HTB-82 7 days after infection with an MOI of 5 [8]. Others examined the effects of Seneca Valley virus, NTX-010, against RMS. Two of the four RMSs had an IC_{50} less than 1 virus particle per cell, and NTX-010 inhibited the growth of four alveolar RMS xenografts *in vivo* [25]. Data regarding the ability of oHSV to target human RMS are sparse. Currier and colleagues studied the effects of a first-generation mutated HSV (NV-1020) upon two RMS cell lines. They found that with multiple injections of virus, the growth of both ARMS and ERMS xenografts was significantly decreased [26]. Pressey et al. demonstrated that ARMS and ERMS cell lines contained myogenically primitive cells marked by CD133 that had cancer stem cell features and were resistant to several chemotherapy agents but were sensitive to oHSV *in vitro* [27]. These previous studies supported our investigations of the oHSV M002 in RMS.

Although virotherapy alone may be a viable therapeutic option for RMS, modifications, such as the addition of exogenous cytokines, could further contribute to the antitumor effects. The oHSV utilized in these studies, M002, was encoded with the gene for mIL-12 [9], and the levels of mIL-12 that were produced by both cell lines were over several nanograms per milliliter. IL-12 is best known as a cytotoxic T-lymphocyte and NK cell activator but also has antitumor effects on RMS. Low serum levels of IL-12 have been correlated with advanced disease, decreased response to chemotherapy, and poor outcome in children with soft tissue sarcomas [28]. Schilbach and others utilized humanized mice to study the effects of IL-12 administration upon human RMS and showed that treatment with an antibody–IL-12 fusion protein arrested cancer cell proliferation and induced myogenic differentiation in the tumors [29]. In the current studies, we investigated oHSV on human RMS cell lines, thereby requiring the use of immunodeficient mice. We were not able to determine the immunologic effects of IL-12 in these xenografts because these mice have negligible immune cells. The precise contribution of IL-12 to the effects of oHSV seen upon RMS cell lines in these studies will certainly be the subject of future investigations.

A novel aspect of the current data is the documentation that both ARMS and ERMS express the CD111 viral entry molecule, lending credence to translating this therapy to the clinical setting. Another important finding was that both ARMS and ERMS cell lines have multiple oHSV viral entry receptors present. Although the expression of CD111 in RMS cell lines has been documented [27], to our knowledge, the demonstration of other important HSV entry receptors has not been previously reported in the literature for these cell lines. The relative expression of these receptors did not significantly affect the ability of M002 to infect the cells. For example, CD111 expression was less in the SJCRH30 compared with the RD cell line, but single and multistep viral infection studies demonstrated similar if not improved infection in the SJCRH30 compared with the RD cell line. In addition, despite lower levels of CD111 protein in the SJCRH30 cell line, M002 was still very

effective at cell killing, and this may be due to the availability of other viral entry proteins such as CD112 and syndecan-2. These findings are consistent with those seen recently with neuroblastoma. Wang and colleagues found that the sensitivity of neuroblastoma cell lines to and infectivity of HSV1716 were not dependent upon the entry proteins or even viral entry itself [19].

We investigated the activation of STAT1 and p38 MAPK as potential mediators of HSV sensitivity. Activation of STAT1 did not increase significantly after virus infection, whereas p38 MAPK activation did increase after treatment. These features have been shown to be favorable for HSV infection by our group and other investigators [21,23,24] and may at least partially explain the sensitivity of the RMS cell lines to M002.

The current studies showed that combining low-dose ionizing radiation with the administration of M002 enhanced the inhibitory effects of M002 on RMS xenograft tumor growth. Previous authors have noted that radiotherapy acts synergistically with other oHSVs [30–33]. Chung and colleagues reported that combining ionizing radiation with R7020 recombinant HSV caused a greater reduction in hepatoma xenografts than either radiation or virus alone [34]. Andusumulli and colleagues showed that oHSV NV1066 when combined with 5-Gy external beam radiation significantly reduced H1299 lung xenograft tumors when compared with either modality alone [32]. In translating this therapy to the clinical setting, our current findings are exceedingly relevant. Radiotherapy is currently included in the treatment regimen for RMS, and the findings from this study demonstrated that combining both modalities for upfront therapy may allow for significant dose reduction in both therapies, leading to potentially decreased therapy-related toxicities. In recurrent disease, tumors may be accessible by radiologic-guided percutaneous interventions, allowing for easier repeated dosing of the virus. Finally, studies are currently being conducted investigating the efficacy of systemic administration of oHSV.

The trends in median xenograft tumor weights were similar to the trends noted in tumor volumes. The final weight of the xenografts from the SJCRH30 cell line treated with M002 and XRT was significantly different from that of xenografts treated with vehicle and XRT but not vehicle alone. This finding may be secondary to the timing of the determination of the weight of the xenografts. The xenografts were weighed at the time of euthanasia, which was dictated by tumor volume reaching IACUC parameters.

In summary, in these studies, we have shown for the first time that multiple injections of oHSV M002 to human xenograft models of RMS resulted in a significant decrease in tumor growth, and radiation augmented this effect. Other novel aspects of this study were the demonstration that multiple oHSV entry molecules were present in the RD and SJCRH30 cell lines and that human RMS tumor specimens express CD111, a key HSV entry molecule. These findings suggest that the humanized form of oHSV, M032, which is currently being studied in a phase I trial in adults with recurrent glioblastoma (clinicaltrials.gov identifier NCT02062827), may have therapeutic potential for these difficult-to-treat pediatric solid tumors.

Supplementary data to this article can be found online at http://dx.doi.org/10.1016/j.tranon.2016.07.008.

Acknowledgements

This work was funded in part by a grant from the National Cancer Institute (T32CA091078; A. M. W., L. L. S., E. F. G). The content of this manuscript was solely the responsibility of the authors and does not necessarily represent the official views of the National Cancer Institute.

References

[1] Rodeberg D and Paidas C (2006). Childhood rhabdomyosarcoma. *Semin Pediatr Surg* **15**, 57–62.

[2] Crist WM, Garnsey L, Beltangady MS, Gehan E, Ruymann F, Webber B, Hays DM, Wharam M, and Maurer HM (1990). Prognosis in children with rhabdomyosarcoma: a report of the Intergroup Rhabdomyosarcoma Studies I and II. Intergroup Rhabdomyosarcoma Committee. *J Clin Oncol* **8**, 443–452.

[3] Rudzinski ER, Anderson JR, Hawkins DS, Skapek SX, Parham DM, and Teot LA (2015). The World Health Organization classification of skeletal muscle tumors in pediatric rhabdomyosarcoma: a report from the Children's Oncology Group. *Arch Pathol Lab Med* **139**, 1281–1287.

[4] HaDuong JH, Martin AA, Skapek SX, and Mascarenhas L (2015). Sarcomas. *Pediatr Clin North Am* **62**, 179–200.

[5] Arndt CA and Crist WM (1999). Common musculoskeletal tumors of childhood and adolescence. *N Engl J Med* **341**, 342–352.

[6] Dasgupta R and Rodeberg DA (2012). Update on rhabdomyosarcoma. *Semin Pediatr Surg* **21**, 68–78.

[7] Burke MJ, Ahern C, Weigel BJ, Poirier JT, Rudin CM, Chen Y, Cripe TP, Bernhardt MB, and Blaney SM (2015). Phase I trial of Seneca Valley Virus (NTX-010) in children with relapsed/refractory solid tumors: a report of the Children's Oncology Group. *Pediatr Blood Cancer* **62**, 743–750.

[8] He S, Li P, Chen CH, Bakst RL, Chernichenko N, Yu YA, Chen N, Szalay AA, Yu Z, and Fong Y, et al (2012). Effective oncolytic vaccinia therapy for human sarcomas. *J Surg Res* **175**, e53–e60.

[9] Parker JN, Gillespie GY, Love CE, Randall S, Whitley RJ, and Markert JM (2000). Engineered herpes simplex virus expressing IL-12 in the treatment of experimental murine brain tumors. *Proc Natl Acad Sci U S A* **97**, 2208–2213.

[10] Chou J, Kern ER, Whitley RJ, and Roizman B (1990). Mapping of herpes simplex virus-1 neurovirulence to gamma 134.5, a gene nonessential for growth in culture. *Science* **250**, 1262–1266.

[11] Friedman GK, Moore BP, Nan L, Kelly VM, Etminan T, Langford CP, Xu H, Han X, Markert JM, and Beierle EA, et al (2016). Pediatric medulloblastoma xenografts including molecular subgroup 3 and CD133+ and CD15+ cells are sensitive to killing by oncolytic herpes simplex viruses. *Neuro Oncol* **18**, 227–235.

[12] Gillory LA, Megison ML, Stewart JE, Mroczek-Musulman E, Nabers HC, Waters AM, Kelly V, Coleman JM, Markert JM, and Gillespie GY, et al (2013). Preclinical evaluation of engineered oncolytic herpes simplex virus for the treatment of neuroblastoma. *PLoS One* **8**, e77753.

[13] Megison ML, Gillory LA, Stewart JE, Nabers HC, Mroczek-Musulman E, Waters AM, Coleman JM, Kelly V, Markert JM, and Gillespie GY, et al (2014). Preclinical evaluation of engineered oncolytic herpes simplex virus for the treatment of pediatric solid tumors. *PLoS One* **9**, e86843.

[14] Beierle EA, Ma X, Stewart JE, Nyberg C, Trujillo A, Cance WG, and Golubovskaya VM (2010). Inhibition of focal adhesion kinase decreases tumor growth in human neuroblastoma. *Cell Cycle* **9**, 1005–1015.

[15] Advani SJ, Sibley GS, Song PY, Hallahan DE, Kataoka Y, Roizman B, and Weichselbaum RR (1998). Enhancement of replication of genetically engineered herpes simplex viruses by ionizing radiation: a new paradigm for destruction of therapeutically intractable tumors. *Gene Ther* **5**, 160–165.

[16] Huertas-Martínez J, Rello-Varona S, Herrero-Martín D, Barrau I, García-Monclús S, Sáinz-Jaspeado M, Lagares-Tena L, Núñez-Álvarez Y, Mateo-Lozano S, and Mora J, et al (2014). Caveolin-1 is down-regulated in alveolar rhabdomyosarcomas and negatively regulates tumor growth. *Oncotarget* **5**, 9744–9755.

[17] Friedman GK, Langford CP, Coleman JM, Cassady KA, Parker JN, Markert JM, and Yancy Gillespie G (2009). Engineered herpes simplex viruses efficiently infect and kill CD133+ human glioma xenograft cells that express CD111. *J Neurooncol* **95**, 199–209.

[18] Krummenacher C, Baribaud F, Ponce de Leon M, Baribaud I, Whitbeck JC, Xu R, Cohen GH, and Eisenberg RJ (2004). Comparative usage of herpesvirus entry mediator A and nectin-1 by laboratory strains and clinical isolates of herpes simplex virus. *Virology* **322**, 286–299.

[19] Wang PY, Swain HM, Kunkler AL, Chen CY, Hutzen BJ, Arnold MA, Streby KA, Collins MH, Dipasquale B, and Stanek JR, et al (2016). Neuroblastomas

vary widely in their sensitivities to herpes simplex virotherapy unrelated to virus receptors and susceptibility. *Gene Ther* **23**, 135–143.

[20] Bacsa S, Karasneh G, Dosa S, Liu J, Valyi-Nagy T, and Shukla D (2011). Syndecan-1 and syndecan-2 play key roles in herpes simplex virus type-1 infection. *J Gen Virol* **92**, 733–743.

[21] Mezhir JJ, Advani SJ, Smith KD, Darga TE, Poon AP, Schmidt H, Posner MC, Roizman B, and Weichselbaum RR (2005). Ionizing radiation activates late herpes simplex virus 1 promoters via the p38 pathway in tumors treated with oncolytic viruses. *Cancer Res* **65**, 9479–9484.

[22] Advani SJ, Markert JM, Sood RF, Samuel S, Gillespie GY, Shao MY, Roizman B, and Weichselbaum RR (2011). Increased oncolytic efficacy for high-grade gliomas by optimal integration of ionizing radiation into the replicative cycle of HSV-1. *Gene Ther* **18**, 1098–1102.

[23] Mahller YY, Sakthivel B, Baird WH, Aronow BJ, Hsu YH, Cripe TP, and Mehrian-Shai R (2008). Molecular analysis of human cancer cells infected by an oncolytic HSV-1 reveals multiple upregulated cellular genes and a role for SOCS1 in virus replication. *Cancer Gene Ther* **15**, 733–741.

[24] Friedman GK, Nan L, Haas MC, Kelly VM, Moore BP, Langford CP, Xu H, Han X, Beierle EA, and Markert JM, et al (2015). $\gamma_1$34.5-deleted HSV-1-expressing human cytomegalovirus IRS1 gene kills human glioblastoma cells as efficiently as wild-type HSV-1 in normoxia or hypoxia. *Gene Ther* **22**, 348–355.

[25] Morton CL, Houghton PJ, Kolb EA, Gorlick R, Reynolds CP, Kang MH, Maris JM, Keir ST, Wu J, and Smith MA (2010). Initial testing of the replication competent Seneca Valley virus (NTX-010) by the pediatric preclinical testing program. *Pediatr Blood Cancer* **55**, 295–303.

[26] Currier MA, Adams LC, Mahller YY, and Cripe TP (2005). Widespread intratumoral virus distribution with fractionated injection enables local control of large human rhabdomyosarcoma xenografts by oncolytic herpes simplex viruses. *Cancer Gene Ther* **12**, 407–416.

[27] Pressey JG, Haas MC, Pressey CS, Kelly VM, Parker JN, Gillespie GY, and Friedman GK, et al (2013). CD133 marks a myogenically primitive subpopulation in rhabdomyosarcoma cell lines that are relatively chemoresistant but sensitive to mutant HSV. *Pediatr Blood Cancer* **60**, 45–52.

[28] Bien E, Krawczyk M, Izycka-Swieszewska E, Trzonkowski P, Kazanowska B, Adamkiewicz-Drozynska E, and Balcerska A (2013). Deregulated systemic IL-10/IL-12 balance in advanced and poor prognosis paediatric soft tissue sarcomas. *Biomarkers* **18**, 204–215.

[29] Schilbach K, Alkhaled M, Welker C, Eckert F, Blank G, Ziegler H, Sterk M, Müller F, Sonntag K, and Wieder T, et al (2015). Cancer-targeted IL-12 controls human rhabdomyosarcoma by senescence induction and myogenic differentiation. *Oncoimmunology* **4**, e1014760.

[30] Dai MH, Zamarin D, Gao SP, Chou TC, Gonzalez L, Lin SF, and Fong Y (2010). Synergistic action of oncolytic herpes simplex virus and radiotherapy in pancreatic cancer cell lines. *Br J Surg* **97**, 1385–1394.

[31] Adusumilli PS, Chan MK, Hezel M, Yu Z, Stiles BM, Chou TC, Rusch VW, and Fong Y (2007). Radiation-induced cellular DNA damage repair response enhances viral gene therapy efficacy in the treatment of malignant pleural mesothelioma. *Ann Surg Oncol* **14**, 258–269.

[32] Adusumilli PS, Stiles BM, Chan MK, Chou TC, Wong RJ, Rusch VW, and Fong Y (2005). Radiation therapy potentiates effective oncolytic viral therapy in the treatment of lung cancer. *Ann Thorac Surg* **80**, 409–416.

[33] Blank SV, Rubin SC, Coukos G, Amin KM, Albelda SM, and Molnar-Kimber KL (2002). Replication-selective herpes simplex virus type 1 mutant therapy of cervical cancer is enhanced by low-dose radiation. *Hum Gene Ther* **13**, 627–639.

[34] Chung SM, Advani SJ, Bradley JD, Kataoka Y, Vashistha K, Yan SY, Markert JM, Gillespie GY, Whitley RJ, Roizman B, and Weichselbaum RR (2002). The use of a genetically engineered herpes simplex virus (R7020) with ionizing radiation for experimental hepatoma. *Gene Ther* **9**, 75–80.